

1 **Hectorites syntheses in different heating**
2 **conditions and their evaluation as soot**
3 **combustion catalysts after impregnation with**
4 **copper.**~~**Evaluation of copper/hectorites as soot**~~
5 ~~**combustion catalysts.**~~

6
7
8
9 T. Sánchez^a, F.B. Gebretsadik^a, P. Salagre^a, Y. Cesteros^a, N. Guillén-Hurtado^b, A.
10 García-García^b, A. Bueno-López^{b,*}.

11
12
13 ^aDepartment of Physical and Inorganic Chemistry. University of Rovira I Virgili,
14 C/ Marcel·lí Domingo s/n, 43007 Tarragona, SPAIN (e-mail addresses: ~~xxxxxx~~
15 ~~xxxxxx~~; cesteros@quimica.urv.es; pilar.salagre@urv.cat)

16
17 ^bDepartment of Inorganic Chemistry. University of Alicante. Ap. 99, E-03080 Alicante.
18 SPAIN. (e-mail addresses: noelia.guillen@ua.es; a.garcia@ua.es; agus@ua.es).

19
20
21 **Abstract**

22
23 Two microporous hectorites were prepared by conventional and microwave heating, and
24 a delaminated mesoporous hectorite by an ultrasound-assisted synthesis, and these three
25 hectorites were impregnated with copper. The characterization techniques used were
26 XRD, N₂ adsorption, TEM and H₂ reduction after selective surface copper oxidation by
27 N₂O (to determine copper dispersion). The catalytic activity for soot combustion of
28 both the copper-free and the copper-containing hectorites was tested under a gas
29 mixture of 500 ppm NO_x/5% O₂/N₂ (and 5% O₂/N₂ in particular cases), evaluating their
30 stability through three consecutive soot combustion experiments.

31 The delaminated hectorite achieved the highest surface area (353 m²/g) and also the
32 highest dispersion of copper, and this copper-containing catalyst was the most active
33 for soot combustion among those prepared and tested in this study. It has been also
34 concluded that the Cu/hectorite-catalyzed soot combustion mechanism is based on the
35 activation of the O₂ molecule and not on the NO₂-assisted soot combustion.

36
37
38 **Keywords:** copper catalysts, delaminated hectorites, diesel soot, soot combustion
39 mechanism.

40
41 * Corresponding author: Tel.: +34 600948665; e-mail address: agus@ua.es (A. Bueno-López).
42 Fax: +34 965903454. e-mail: agus@ua.es

Con formato: Resaltar

Con formato: Inglés (Estados Unidos),
Resaltar

Con formato: Resaltar

43

44

45
46 **1. Introduction.**

47
48 Soot particles produced by diesel engines have negative effects on health, and
49 their emission must be controlled and is currently regulated. In order to avoid soot
50 emissions, soot particles are collected on filters placed in the diesel exhausts, which
51 must be periodically regenerated by soot combustion. Diesel gas exhausts ~~are composed~~
52 consist of a high proportion of O₂, CO₂ and H₂O, and in lower concentration NO_x, CO
53 and unburned hydrocarbons, and soot must be combusted in such particular
54 environment.

Con formato: Inglés (Estados Unidos)

55 In a diesel exhaust there are three oxidizing gases that can potentially react with
56 soot: O₂, NO and NO₂. Typically, only NO and O₂ are emitted by the engine, and some
57 soot combustion catalysts (like Pt in the commercially available CRT system, for
58 instance (van Setten ~~B.A.A.L~~-et al., 2001; Fino ~~D~~-et al., 2008) accelerate the oxidation
59 of NO to NO₂, which is much more oxidizing than NO and O₂.

Con formato: Inglés (Estados Unidos)

60 A number of catalysts have been reported to accelerate the combustion of soot,
61 such as noble metals (Sánchez ~~B.S~~-et al., 2009; Shimokawa ~~H~~-et al., 2012), alkali metals
62 (~~Aneggi et al., 2008~~; Peralta ~~M.A.~~-et al., 2011; ~~Aneggi E. et al., 2008~~), transition metals
63 and metal oxides among others (Neeft J.P.A-~~et al.~~, 1996; López-Suárez ~~F.E~~-et al.,2008,
64 2009; Guillén-Hurtado ~~N~~-et al., 2012). Among these potential catalysts, copper oxide
65 appears as an interesting solution due to its moderate activity but low prize.

Con formato: Inglés (Estados Unidos)

66 It is known that the catalyst support (ceria, alumina, silica, etc.) affects in some
67 cases the activity of the main active component of a soot combustion catalyst. However,
68 as far as we know, the soot combustion activity of hectorites s either as catalyst or as
69 catalytic support has not been reported yet.

70 Hectorite is a trioctahedral 2:1 ~~mineral-clay~~clay mineral, belonging to the
71 smectites group, with formula $(\text{Si}_{8.0})[\text{Mg}_{6.0-x}\text{Li}_x](\text{OHF})_4\text{O}_{20}\text{M}^{n+}_{x/n}\cdot m\text{H}_2\text{O}$, where some
72 substitution of ~~Mg(II) by Li(I) in the Octahedral (O_h) sheet~~ Mg^{2+} by Li^+ in the octahedral
73 (O) sheet causes the negative charge of layers. This charge is compensated by interlayer
74 exchangeable cations. ~~When these cations are exchanged by transition metal cations~~
75 ~~(Ni^{2+} , Pd^{2+} , Cu^{2+}),~~ metallic nanoparticles of metals with catalytic activity, like, Ni^0 ,
76 Pd^0 or Cu^0 among others, can be obtained, ~~after reduction,~~ in the interlayer space by
77 ionic exchange and further reduction. Hectorites can be used for nanocomposites
78 preparation, in ionic adsorption and in heterogeneous catalysis among other applications
79 (Varma, 2002; Casagrande et al., 2005; Liu-X. et al., 2005; Xue-S et al., 2008;
80 Casagrande M. et al., 2005; Varma R.S. 2002). Applications of smectites as catalysts
81 are very extensive, especially in acid and oxidation reactions (Varma 2002; Casagrande
82 M. et al., 2005; Varma R.S. 2002). Additionally, they have been also widely used as
83 supports of metal catalysts leading to significant results, for example, in the
84 hydrogenation of styrene oxide to 2-phenylethanol with hectorites and saponites-
85 supported nickel catalysts (Vicente I-et al., 2011-a, 2011b) or in the hydrogenolysis of
86 glycerol to 1,2-propanediol with delaminated hectorites-supported copper catalysts
87 ~~based on copper supported on delaminated hectorites~~-(Sánchez-T. et al., 2012).

Con formato: Superíndice

88 Although clays can be found in nature, better composition, reproducibility and
89 higher surface area are necessary in order to improve their catalytic
90 ~~applications~~performance. Preparation of synthetic clay minerals and delamination could
91 solve the limitations of natural clays.~~Synthetic preparation of clays and delamination~~
92 ~~could solve these requirements, respectively.~~ Delaminated hectorites can be
93 ~~synthesised~~synthesized using adding quaternary ammonium salts during the
94 hydrothermal treatment, as proposed by Iwasaki-T. et al. (1998) and by Sánchez et al.

95 | (2012), or using polymers, as proposed by Carrado et al. (1999). Typical methods for
96 | preparing supported metal catalysts include impregnation, solid blend and modification
97 | of hectorite by cation exchange. Depending on the method, different metal dispersions
98 | and support-metal interactions can be obtained ([Meister et al., 1995](#); ~~Vicente-I. et al.,~~
99 | ~~2011-a, 2011b~~ ; ~~Sánchez T. et al., 2012~~; ~~Meister A. et al., 1995~~).

100 | Taking this background into account, the goal of this study is to [prepare different](#)
101 | [hectorite samples and to](#) evaluate the potential of [these](#) hectorites as soot combustion
102 | catalysts in a gas mixture with NO_x and O₂, either as catalyst or as copper support.

104 | **2. Experimental.**

106 | 2.1. Catalyst preparation.

108 | 2.1.1. Hectorite samples.

110 | Two hectorites, which are referred to as HC and HMw, were prepared according
111 | to the procedures reported by Granquist-~~W.T.~~ and Pollack-~~S.S.~~ (1959) and Vicente-~~I.~~ et
112 | al. (2009). In both methods brucite sheets were proposed to act as crystallization nuclei
113 | of hectorite. Preparation was carried out as follows: a slurry (3 ~~wt.mass~~ % solids)
114 | containing SiO₂ (Aerosil 380 from Degussa), fresh brucite Mg(OH)₂ (synthesized by
115 | dropping a 10 M ammonia solution onto MgCl_{2(aq)}), and LiF (99.9% from Sigma-
116 | Aldrich), in a molar ratio SiO₂:Mg(OH)₂:LiF of 8:6:2 was vigorously stirred for 1 h.

117 | -Then, one [of the samples, which is referred to as “HMw”](#), was aged [by](#)
118 | [microwaves \(in a Milestone Ethos Touch Control equipment\) at 120°C for 8 h under](#)
119 | [magnetic stirring. The treatment was performed by in a 85 mL autoclaving in](#)-Teflon

120 ~~autoclave reactors of 85 mL in a laboratory microwave equipment (Milestone Ethos~~
121 ~~Touch Control) at 120 °C for 8 h under magnetic stirring (HMw). The second~~Another
122 sample, which is referred to as “HC”, was aged ~~in~~ within a Teflon autoclave by
123 conventional thermal heating inside a conventional oven (HC) at 120 °C for 8 days, in
124 order to compare the conventional aging with the microwave hydrothermal treatment.

125 A delaminated hectorite~~third sample, which is~~ referred to as HD₁ was also
126 prepared, ~~in order to obtain a delaminated hectorite,~~ according to the method reported
127 by Iwasaki ~~T.~~ et al. (1998), which was and later further modified by Sánchez ~~T.~~ et al.
128 (2012) by introducing the use of using ultrasounds for ~~the~~ homogenization of the initial
129 precursors suspension. ~~The molar ratio of reagents was Si:Mg:Li= 8:5.2:0.8.~~ 8.73 g of
130 an acidified sodium silicate solution (SiO₂ 27%, d. 1.39 g/cm³, Sigma-Aldrich) was
131 mixed with the appropriate amounts of MgCl₂ and LiF to obtain a molar ratio of
132 Si:Mg:Li reagents of 8:5.2:0.8. Then, a LiOH solution was added until pH=12. The
133 resulting suspension was homogenized for 15 min in an ultrasound bath, washed and
134 dried. Then, the solid was suspended in water and mixed with
135 trimethyldodecylammonium chloride (AQ) (98%, Sigma-Aldrich) in a molar ratio
136 Li:AQ= 1:1. The suspension was submitted to a hydrothermal treatment in a
137 conventional Teflon autoclave at 180 °C for 1 h. Afterwards, the precipitated sample
138 was ~~separated~~ filtered and calcined to 620 °C for 75 min (HD).

139

140 2.1.2. Cu/hectorite samples.

141

142 Cu/hectorite samples were prepared by impregnation according to the method
143 described by Sánchez ~~T.~~ et al. (2012). Impregnated hectorites were prepared mixing 1.5
144 g of support (HMw, HC or HD) with a 15 ~~wt~~ mass % copper nitrate ethanol solution

145 | under ultrasounds for 15 min, in order to obtain around 40 ~~wt-mass~~ % copper after
146 | solvent evaporation, calcination, and reduction under pure hydrogen. Impregnated
147 | hectorites ~~are referred to have been named~~ as Cu/HMw, Cu/HC and Cu/HD.

148 |

149 | 2.2. Characterization techniques.

150 |

151 | 2.2.1. X-Ray Diffraction (XRD).

152 |

153 | XRD measurements were made using a Siemens D5000 diffractometer (Bragg–
154 | Brentano parafocusing geometry and vertical θ – θ goniometer) fitted with a curved
155 | graphite diffracted-beam monochromator and diffracted-beam Soller slits, a 0.06°
156 | receiving slit, and scintillation counter as a detector. The angular 2θ diffraction range
157 | was between 2 and 70° . The samples were ~~dusted-milled and placed on~~ a low
158 | background ~~signal~~ Si(510) sample holder. The data were collected with an angular step
159 | of 0.05° at 3 s per step and ~~by~~ sample rotation. $\text{CuK}\alpha$ radiation was obtained from a
160 | copper X-ray tube operated at 40 kV and 30 mA. The X-ray diffractograms ~~was-were~~
161 | analyzed using the program TOPAS 3.0. Reflection (001) was selected to determine the
162 | basal spacing ~~of the samples~~(Sánchez et al., 2012) and ~~r~~Reflection (060) was used to
163 | calculate the crystallite size of the sample ~~sheets~~layers.

164 |

165 | 2.2.2. N_2 adsorption-desorption.

166 |

167 | N_2 adsorption-desorption isotherms were recorded at -196°C using a
168 | Micromeritics ASAP 2000 surface analyzer. Prior to analysis samples were outgassed at
169 | 150°C . Specific surface areas were calculated from BET method.

170

171 2.2.3. Transmission Electron Microscopy (TEM).

172

173 Transmission electron micrographs were obtained with a JEOL 1011
174 transmission microscope operating at an accelerating voltage of 100 kV and
175 magnification values at 300000.

176

177 2.2.4. Temperature-Programmed Reduction (TPR).

178

179 Copper dispersion was determined by selective temperature-programmed
180 reduction of surface copper following the method described by Gervasini~~A.~~ and
181 Bennici~~S.~~ (2005). These experiments were carried out in a Micromeritics device, model
182 Pulse ChemiSorb 2705. 100 mg of catalyst were heated at 10-°C/min from 25 to 400-°C
183 under a 5% H₂/Ar flow (15 ml/min), holding the maximum temperature for 30 min. The
184 H₂ consumption was monitored with a TCD detector. Then, the selective oxidation of
185 the surface copper ~~surface~~ to Cu₂O was performed under 0.53% N₂O/Ar flow (15
186 ml/min) at 50-°C for 1 h. Surface Cu₂O ~~surface~~ was further reduced with 5% H₂/Ar (15
187 ml/min) by raising the temperature at 20-°C/min from 25 to 900-°C, following the H₂
188 consumption with the TCD detector. The potential interference of H₂ consumption by
189 the supports was ruled out in experiments performed with the supports (without copper).

190 Surface copper was determined considering the stoichiometry of the reaction:



192 “Dispersion (%)” was calculated as the ratio between the amount of surface
193 copper and total copper in the catalyst:

194
$$\text{Dispersion (\%)} = \frac{\text{Cu}_{\text{surface}}}{\text{Cu}_{\text{total}}} \cdot 100$$

195 A CuO sample (supplied by Micromeritics) was used as reference to quantify H₂
196 consumption.

197

198 2.3. Catalytic activity tests.

199

200 Catalytic tests were performed in a tubular quartz reactor coupled to specific
201 NDIR-UV gas analyzers for CO, CO₂, NO, NO₂ and O₂ monitoring. 20 mg of soot and
202 80 mg of the selected hectorite sample were mixed in the so-called loose contact
203 conditions (Neef ~~J.P.A.~~ et al., 1996) and diluted with SiC to avoid pressure drop and
204 favor heat transfer. Uncatalysed combustion experiments were also performed under the
205 same conditions but only with soot. The model soot used was carbon black from
206 Evonik-Degussa (Printex-U), with 92.2% C, 0.6% H, 0.2% N, and 0.4% S. The ash and
207 adsorbed hydrocarbon percentages were <0.1 and 5.2%, respectively, and the BET
208 surface area was 95 m²/g. The gas mixtures used contained either 500 ppm NO_x/5%
209 O₂/N₂ or 5% O₂/N₂, and the gas flow was fixed at 500 ml/min in all cases (GHSV =
210 30000 h⁻¹). The experimental set-up was designed to minimize the uncatalysed
211 oxidation of NO to NO₂ on the gas stream.

212 The catalytic tests were carried out in temperature programmed conditions
213 followed by an isothermal step, that is, once the gas mixture is fed to the reactor and all
214 lectures of the gas analyzers were stable, the temperature was increased from room
215 temperature until 600°C at 10°C/min, and the maximum temperature was maintained
216 for 30 minutes. Three consecutive soot combustion experiments were performed with
217 each sample. Once the first soot combustion test was finished, the reactor was cooled
218 down to room temperature under 5% O₂/N₂ gas flow, the used hectorite was mixed
219 again with soot following the procedure previously described in the experimental

220 section, and a second catalytic test was performed. In the same way, a third run was
221 performed with each hectorite sample.

222

223 3. Results and discussion.

224

225 3.1. Characterization of hectorite and Cu/hectorite samples.

226

227 Table 1 shows some characterization data of the hectorite samples. XRD
228 patterns of the three samples were typical of clay minerals, as it is shown in the
229 reference elays materials (Sánchez ~~T~~ et al., 2012). However, reflection (001), related to
230 the layer stacking, was only observed in hectorites HC and HMw (Table 1). The low
231 degree of order stacking in sample HD, related to the absence of reflection (001) in the
232 diffraction pattern (Fig 1), could be associated with delamination, ~~as~~ As confirmed by
233 TEM, ~~since we can observe~~ nano-sized layers are observed, which are aggregated to
234 make mesopores (Fig. 2). In order to evaluate the crystallinity of the layers, crystallite
235 sizes were calculated from (060) reflection using the Scherrer equation (Table 1). The
236 hectorite prepared ~~with~~ by microwaves heating (HMw) showed higher crystallite size
237 (10.5 nm) than that synthesized by conventional heating HC (7.9 nm). This is in
238 agreement with the increase of crystallinity expected for materials prepared with
239 microwaves (Bergadà et al., 2007; Vicente ~~I~~ et al., 2009, 2010; Bergadà O. et al., 2007).
240 Delaminated hectorite, HD, had the lowest crystallite size (6.0 nm). This can be
241 explained by the shorter time of hydrothermal treatment used to prepare this sample (1
242 h).

243 Regarding the BET surface area values (Table 1), mesoporous delaminated
244 hectorite (HD) showed the highest surface area, as expected, in agreement with its

245 delamination observed by TEM (Fig. 1). With respect to porosity, it is important to
246 remark that all synthesized hectorites exhibited adsorption isotherms with contribution
247 of mesoporosity (type IV), but with different hysteresis loop (Sánchez T. et al., 2012).
248 For HC and HMw, hysteresis was type B (following Boer classification (of Boer J.H.
249 1958) (Table 1). Hysteresis type B is associated to lamellar particles that are packed
250 together with formation of open slit-shaped capillaries with parallel walls, whereas
251 hysteresis type D is more characteristic of lamellar particles that are packed without
252 parallel orientation (Sánchez T. et al., 2012). The hysteresis loop of HD was identified
253 as a mix of B and D types, with higher contribution of D (Fig. 3). This agrees with the
254 disorder observed in the lamellar distribution for this sample.

255 Table 2 shows the amount of copper and the dispersion obtained for the
256 Cu/hectorite samples. Dispersion values can be directly related to the surface area of the
257 supports. Thus, delaminated hectorite, which had higher surface area, showed the
258 highest dispersion of copper. Although the dispersion values are low, it is important to
259 remark the significant amount of copper on the surface of the catalysts. This will be
260 later correlated with the catalytic results.

261

262 3.2. Soot combustion tests: catalysts screening.

263

264 Fig. 4 shows the soot conversion profiles obtained during the third soot
265 combustion test performed with each copper-free and copper-containing hectorite in the
266 500 ppm NO_x/5% O₂/N₂ gas flow. The copper-free microporous hectorites (HC and
267 HMw) present null activity as soot combustion catalysts while the mesoporous hectorite
268 (HD) was able to slightly accelerate the combustion reaction. As expected, the copper-
269 containing hectorites were more active than the supports, and among them, the catalyst

270 Cu/HD, prepared with the mesoporous hectorite, was the most active one. The highest
271 amount of surface copper on this catalyst justifies this fact. As a general behavior, the
272 Cu/hectorite catalysts tested were less active than some other soot combustion copper
273 catalysts, such as Cu/alumina (López-Suárez [F.E.](#)-et al., 2008) or Cu/SrTiO₃ perovskites
274 (López-Suárez [F.E.](#)-et al., 2009).

275 The stability of the hectorite supports and Cu/hectorite catalysts was evaluated in
276 three consecutive soot combustion experiments performed with the 500 ppm NO_x/5%
277 O₂/N₂ gas flow. Fig. 5 compiles the time required to achieve 90% soot conversion in
278 each experiment. In all cases, minor differences were noticed among the three
279 consecutive cycles, that is, the soot combustion capacity is not significantly affected
280 under the experimental conditions of these tests (López-Suárez [F.E.](#)-et al., 2008, 2009).

281 One important feature of soot combustion catalysts to be taken into account is
282 the carbon products selectivity, since CO is hazardous and toxic while CO₂ is the
283 desired product. CO selectivity results are compiled in Fig. 6 for all the supports and
284 catalysts tested in three consecutive combustion cycles under 500 ppm NO_x/5% O₂/N₂.
285 The uncatalysed combustion of soot yielded 60% CO, and some of the hectorite
286 samples tested lowered this value. The Cu/hectorite catalysts presented CO selectivity
287 values between 10 and 33%, and among the supports, only HD was able to lower the
288 CO selectivity to around 45%. These results suggest that these Cu/hectorite samples
289 catalyze the oxidation of CO, [which is](#) evolved as primary soot combustion product, to
290 CO₂. This is in agreement with the results obtained with some other soot combustion
291 copper catalysts (López-Suárez [F.E.](#)-et al., 2008, 2009).

292

293 3.3. Soot combustion mechanism.

294

295 In order to analyze the Cu/hectorite-catalyzed soot combustion mechanism, a
296 soot combustion experiment was performed with the most active catalyst among those
297 tested (Cu/HD) ~~with~~ under a 5% O₂/N₂ gas flow. The soot conversion curve obtained in
298 this experiment is plotted in Fig. 7 together with the counterpart curve obtained ~~with~~
299 under 500 ppm NO_x/5% O₂/N₂. Both curves are almost equal, evidencing that NO_x is
300 not playing a key role in the soot combustion mechanism, that is, the NO₂-assisted soot
301 combustion mechanism can be ruled out.

302 Additional information about the soot combustion mechanism was obtained
303 from the NO₂ formation and NO_x removal profiles corresponding to the soot
304 combustion and blank experiments (without soot) performed with the Cu/HD catalyst
305 with 500 ppm NO_x/5% O₂/N₂ (Fig. 8). A little amount of NO_x was chemisorbed on the
306 catalyst during the blank experiment, and the shape of the NO₂ profile obtained in this
307 blank experiment was similar to those typically reported for some other catalysts
308 (López-Suárez ~~F.E.~~ et al., 2008, 2009). The NO₂ level increased with temperature until
309 the thermodynamic equilibrium of the NO₂ formation reaction was achieved. On the
310 contrary, NO_x chemisorption and NO₂ formation were not detected during the soot
311 combustion experiment.

312 These results evidence that the Cu/hectorite catalyst was able to accelerate the
313 oxidation of NO to NO₂ and that NO₂ reacts with soot, since NO₂ was not detected in
314 the soot combustion experiment, but the amount of NO₂ produced was not high enough
315 to affect soot combustion. This suggests that the main role of the Cu/hectorite catalyst is
316 the activation of the O₂ molecule rather than to oxidize NO to NO₂. This could explain
317 why the mesoporous hectorite presents higher activity than the microporous ones, since
318 more contact points with soot particles are expected to exist where the activated oxygen
319 species are transferred to soot.

320

321 **4. Conclusions.**

322

323 In this study, three different hectorites have been prepared and impregnated with
324 copper. The characterization and the catalytic activity for soot combustion of ~~both the~~
325 copper-free and copper-containing hectorites have led to the following conclusions:

326 • Mesoporous delaminated hectorite (HD) presents the lowest crystallite size and
327 the highest surface area, being the only copper free hectorite that slightly accelerates the
328 soot combustion reaction.

329 • Among the Cu/hectorite catalysts, copper supported on a delaminated hectorite
330 (Cu/HD) is the most active one, showing the highest amount of copper on the surface.

331 • Regardless the hectorite support, the Cu/hectorite catalysts decrease the
332 selectivity towards CO formation as soot combustion product and the soot combustion
333 capacity is quite stable after three consecutive soot combustion experiments.

334 • The Cu/hectorite-catalysed soot combustion mechanism is not based on the
335 NO₂-assisted soot combustion, the activation of the O₂ molecule being the main role of
336 these catalysts.

337

338 **Acknowledgments.**

339

340 The authors gratefully acknowledge the financial support of Generalitat
341 Valenciana (Prometeo/2009/047 project) and the Spanish Ministry of Science and
342 Innovation (project CTQ2009-07475 and CTQ2011-24610, which are co-funded by
343 FEDER resources). N. G. H. wishes to thank Generalitat Valenciana her Ph. D. grant
344 within VAL i+d Program.

345

346

347
348 **References**

349 Aneggi E., Leitenburg C., G. Dolcetti, G., Trovarelli A., 2008. Diesel soot combustion
350 activity of ceria promoted with alkali metals. Catal. Today 136, 3-10

351 [Bergadà O., Vicente I., Salagre P., Cesteros Y., Medina F., Sueiras J.E., 2007.](#)
352 Microwave effect during aging on the porosity and basic properties of hydrotalcites.
353 Micropor. Mesopor. Mater. 101, 363-373.

Con formato: Inglés (Estados Unidos)

354 J.H. of Boer, 1958. The Structure and Properties of Porous Materials, Butterwoth,
355 London.

356 [Carrado K.A., Xu L., 1999. Materials with controlled mesoporosity derived from](#)
357 [synthetic polyvinylpyrrolidone-clay composites. Micropor. Mesopor. Mater. 27, 87-94.](#)

Con formato: Inglés (Estados Unidos)

358 Casagrande M., Storaro L., Lenarda M., Rossini S., 2005. Solid acid catalysts from
359 clays: Oligomerization of 1-pentene on Al-pillared smectites. Catal. Commun. 6, 568-
360 572.

361 Fino D., Specchia V., 2008. Open issues in oxidative catalysis for diesel particulate
362 abatement. Powder Technol. 180 64-73.

363 Gervasini A., S. Bennici S., 2005. Dispersion and surface states of copper catalysts by
364 temperature-programmed-reduction of oxidized surfaces (s-TPR). Appl. Catal. A 281,
365 199-205.

366 Granquist W.T., Pollack S.S., 1959. A study of the synthesis of hectorite. Clays Clay
367 Miner. 8, 150-169.

Con formato: Inglés (Estados Unidos)

368 Guillén-Hurtado N., Bueno-López A., García-García A., 2012. Catalytic performances
369 of ceria and ceria-zirconia materials for the combustion of diesel soot under NO_x/O₂
370 and O₂. Importance of the cerium precursor salt. Appl. Catal. A 437-438, 166-172.

371 Iwasaki I., Reinikainen M., Onodera Y., Hayashi H., Ebina T., Nagase T., Torii K.,
372 Kataja K., Chatterjee A., 1998. Use of silicate crystallite mesoporous material as
373 catalysts support for Fischer-Tropsch reaction. Appl. Surf. Sci. 130-132, 845-850.

Con formato: Inglés (Estados Unidos)

Con formato: Inglés (Estados Unidos)

374 Liu X., Breen C., 2005. High temperatura crystalline phases in nylon 6/clay
375 nanocomposites. Macromol. Rapid Commun. 26, 1081-1086.

Con formato: Inglés (Estados Unidos)

376 López-Suárez F.E., Bueno-López A., Illán-Gómez MJ., 2008. Cu/Al₂O₃ catalysts for
377 soot oxidation: Copper loading effect. Appl. Catal. B 84, 651-658.

Con formato: Inglés (Estados Unidos)

378 López-Suárez F.E., Parres-Esclapez S., Bueno-López A., Illán-Gómez M.J., Ura B.,
379 Trawczynski J., 2009. Role of surface and lattice copper species in copper-containing
380 (Mg/Sr)TiO₃ perovskite catalysts for soot combustion. Appl. Catal. B 93, 82-89.

Con formato: Inglés (Estados Unidos)

381 Meister A., Takano N., Chuard T., Graf M., Bernauer K., Stoeckli-evans H., Süss-Fink
382 G., 1995. [Z. Modifizierung von Schichtsilicaten mit sterisch anspruchsvollen](#)
383 [Metallkomplexen, Teil 3: Synthese und Interkalation der planar-quadratischen](#)

Con formato: Inglés (Estados Unidos)

- 384 | [Komplexe \[Cu\(bppep\)\(H₂O\)\]\(ClO₄\)₂ und \[Ni\(bppep\)\(Cl\)\]Cl \(bppep = 2,6-Bis\[1-](#)
385 | [phenyl-1-\(pyridin-2-yl\)ethyl\]pyridin\) in Hectorit](#); Anorg. Allg. Chem. 621, 117-121.
- 386 | Neeft J.P.A, Makkee M., Moulijn J.A 1996.; Metal oxides as catalysts for the oxidation of
387 | soot. Chem. Eng. J. 64, 295-302.
- 388 | [Peralta M.A., Zanuttini M.S., Ulla M.A., Querini C.A., 2011. Activity and stability of](#)
389 | [BaKCo/CeO₂ catalysts for diesel soot oxidation. Appl. Catal. A 399, 161-171.](#)
- 390 | Sánchez B.S., Querini C.A., Miró E.E., 2009. NO_x adsorption and diesel soot
391 | combustion over La₂O₃ supported catalysts containing K, Rh and Pt. Appl. Catal. A
392 | 366, 166-175.
- 393 | Sánchez T., Salagre P., Cesteros Y., Bueno-López A., 2012. Use of delaminated
394 | hectorites as supports of copper catalysts for the hydrogenolysis of glycerol to 1,2-
395 | propanediol. Chem. Eng. J. 179, 302-311.
- 396 | van Setten B.A.A.L., Makkee M., Moulijn J.A., 2001. Science and technology of
397 | catalytic diesel particulate filters. Catal. Rev. 43, 489-564.
- 398 | Shimokawa H., Kurihara Y., Kusaba H., Einagab H., Teraoka Y., 2012. Comparison of
399 | catalytic performance of Ag- and K-based catalysts for diesel soot combustion. Catal.
400 | Today 185, 99-103.
- 401 | Varma R.S., 2002. Clay and clay-supported reagents in organic synthesis. Tetrahedron
402 | 58, 1235-1255.
- 403 | Vicente I., Salagre P., Cesteros Y. 2011. a) Ni nanoparticles supported on microwave-
404 | synthesised hectorite for the hydrogenation of styrene oxide. Appl. Catal. A 408, 31-37.
405 | b) Ni nanoparticles supported on microwave-synthesised saponite for the hydrogenation
406 | of styrene oxide. Appl. Clay Sci. 53, 212-219.
- 407 | [Vicente I., Salagre P., Cesteros Y., Guirado F., Medina, F. Sueiras J.E., 2009. Fast](#)
408 | [microwave synthesis of hectorite. Appl. Clay— Sci. 43, 103-107.](#)
- 409 | [Vicente I., Salagre P., Cesteros Y., Medina F., Sueiras J.E., 2010. Microwave-assisted](#)
410 | [synthesis of saponite. Appl. Clay Sci. 48, 26-31.](#)
- 411 | Xue S., Pinnavaia T.J. 2008. Porous synthetic smectic clay for the reinforcement of
412 | epoxy polymers. Micropor. Mesopor. Mater. 107, 134-140.
- 413

Con formato: Inglés (Estados Unidos), Subíndice

Con formato: Inglés (Estados Unidos)

Con formato: Inglés (Estados Unidos), Subíndice

Con formato: Inglés (Estados Unidos)

Con formato: Inglés (Estados Unidos), Subíndice

Con formato: Inglés (Estados Unidos)

414
415

List of Tables

416
417
418

Table 1. Characterization data from XRD, and N₂ physisorption techniques.

Sample	Basal spacing (Å)	Crystallite size (0 6 0) (nm)	BET surface area (m ² /g)	Hysteresis type
HMw	14.2	10.5	199	B
HC	13.4	7.9	207	B
HD	---	6.0	353	D,B

419
420
421

Table 2. Results of copper dispersion on the different supports.

422
423

Sample	Cu content (wt mass %)	Cu dispersion (%)	g surface Cu /g catalyst x10 ⁻²
Cu/HMw	39.2	4	1.57
Cu/HC	38.7	6	2.32
Cu/HD	40.1	8	3.20

424
425

426
427

Figure captions

428 | **Fig. 1.** X-ray diffraction pattern- of HD hectorite.

429

430 **Fig. 2.** TEM micrograph of HD hectorite.

431

432 **Fig. 3.** N₂ adsorption-desorption isotherm of HD hectorite.

433

434 **Fig.4.** Soot conversion profiles corresponding to the third run performed with each
435 hectorite sample in the 500 ppm NO_x/5% O₂/N₂ gas flow.

436

437 **Fig.5.** Comparison of catalysts during three consecutive soot combustion runs
438 performed in the 500 ppm NO_x/5% O₂/N₂ gas flow.

439

440 **Fig.6.** CO selectivity in soot combustion experiments performed in the 500 ppm
441 NO_x/5% O₂/N₂ gas flow.

442

443 **Fig.7.** Soot combustion experiments performed with Cu/HD catalyst (fresh sample)
444 with 5% O₂/N₂ and 500 ppm NO_x/5% O₂/N₂.

445

446 **Fig.8.** NO₂ formation and NO_x removal in soot combustion and blank experiments
447 performed with Cu/HD catalyst (fresh sample) with 500 ppm NO_x/5% O₂/N₂.

448

449

450

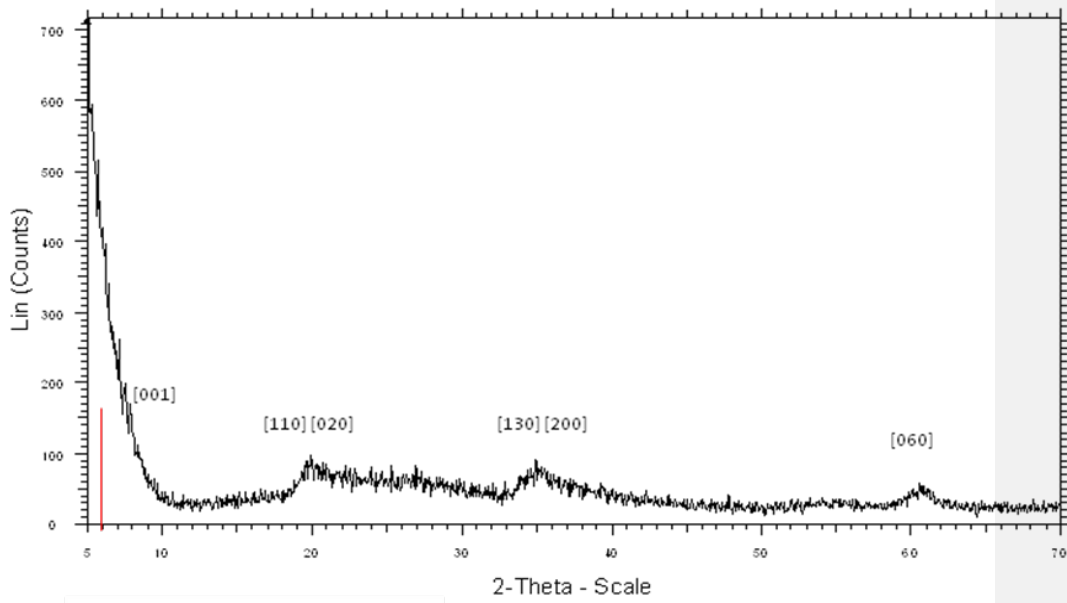
451

452

453

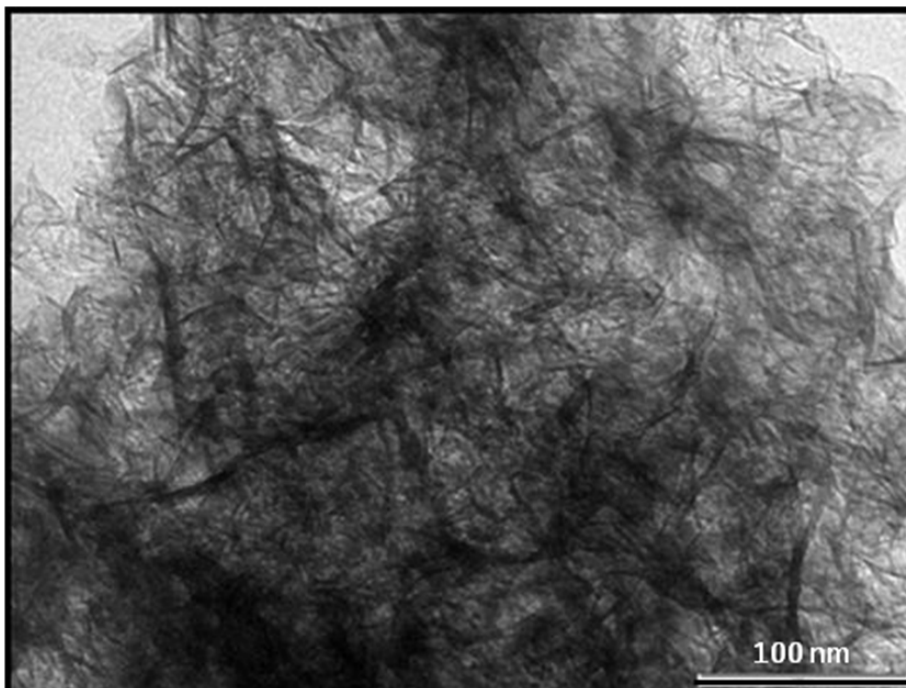
454
455
456
457
458
459
460
461

Figure 1



462
463

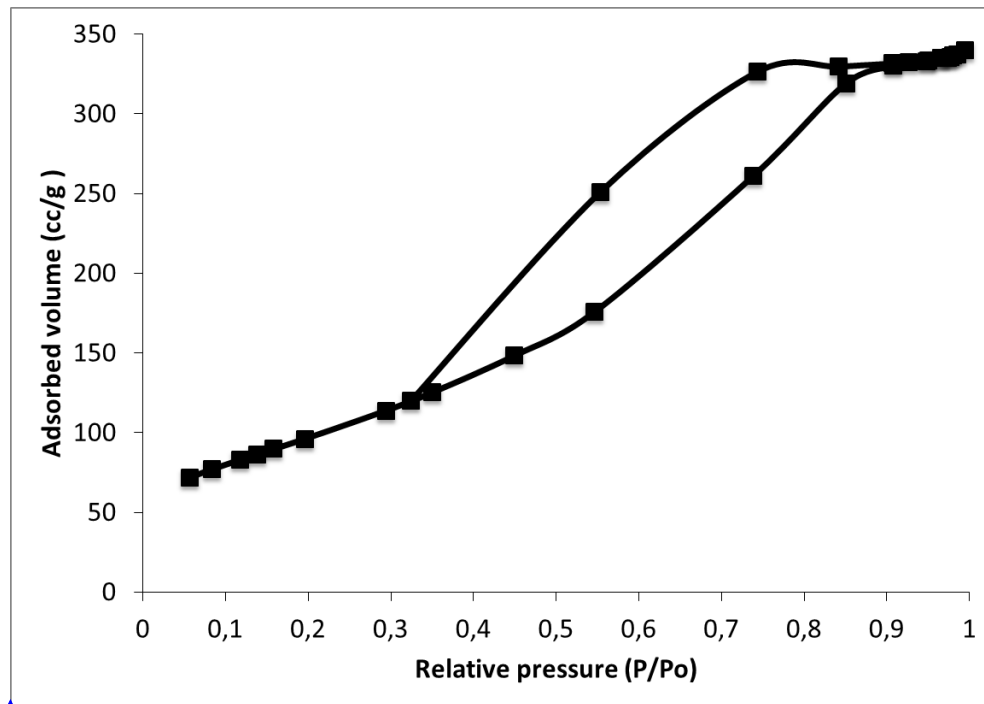
464 **Figure 2**
465
466
467
468
469
470
471
472



473
474
475
476
477
478
479
480
481
482
483
484
485
486
487
488
489
490
491
492

493
494
495
496
497
498
499
500
501

Figure 3

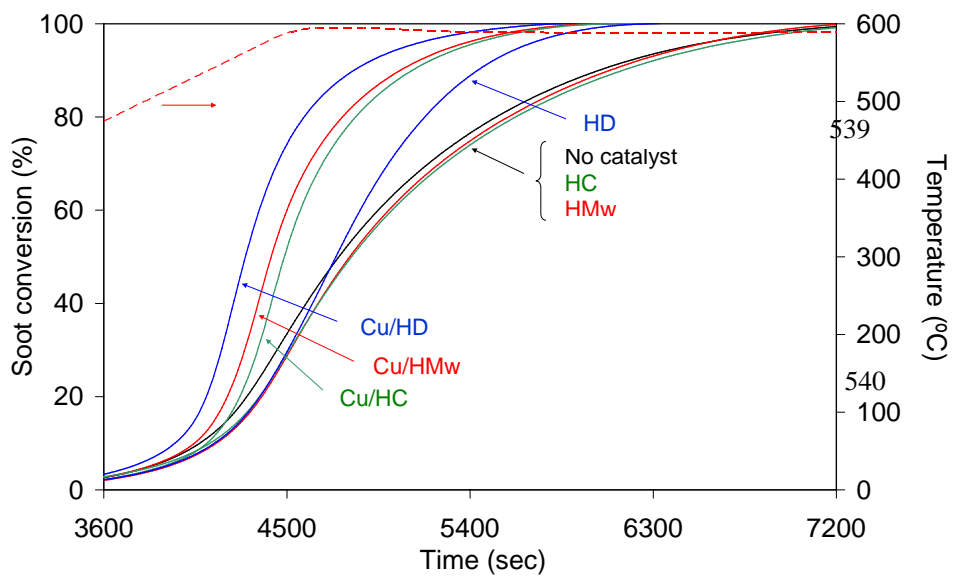


Con formato: Inglés (Estados Unidos)

502
503
504
505
506
507
508
509
510
511
512
513
514
515
516
517
518
519
520
521

522
523
524
525
526
527
528
529
530
531
532
533
534
535
536
537
538

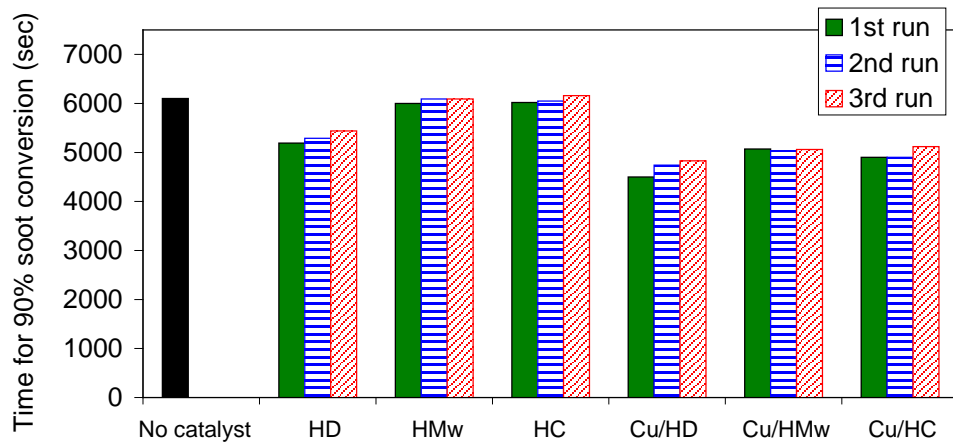
Figure 4



541
542
543
544
545
546

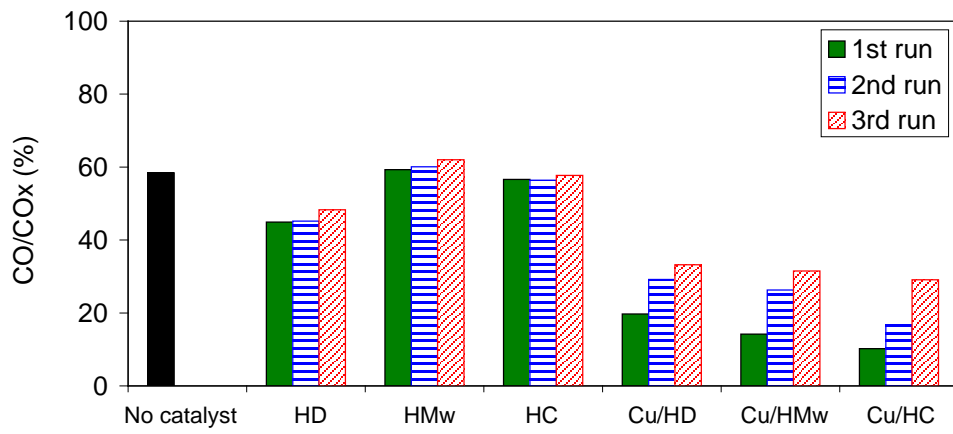
547
548
549
550
551
552
553
554
555
556
557
558
559
560

Figure 5



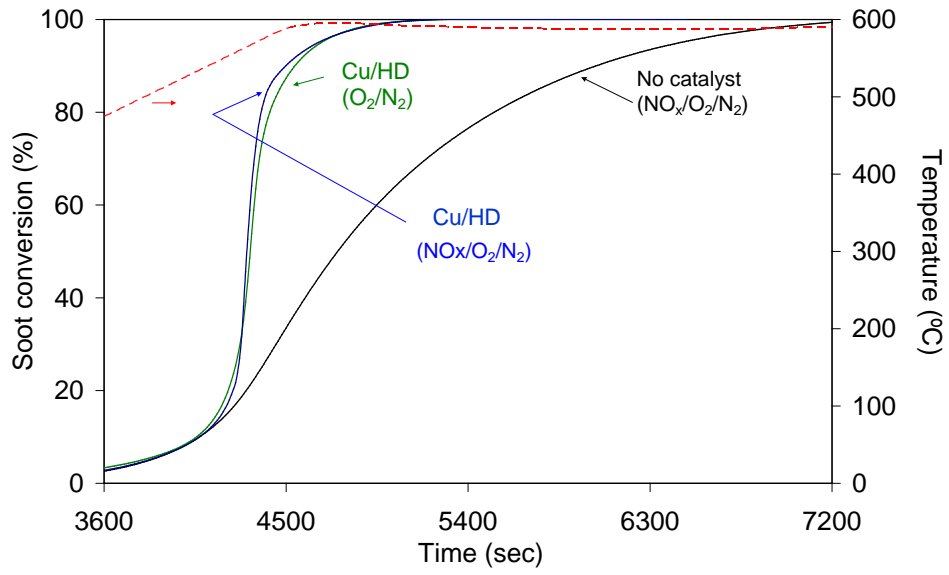
561
562
563
564
565
566
567
568
569
570
571
572
573
574
575

Figure 6



576
577
578
579
580

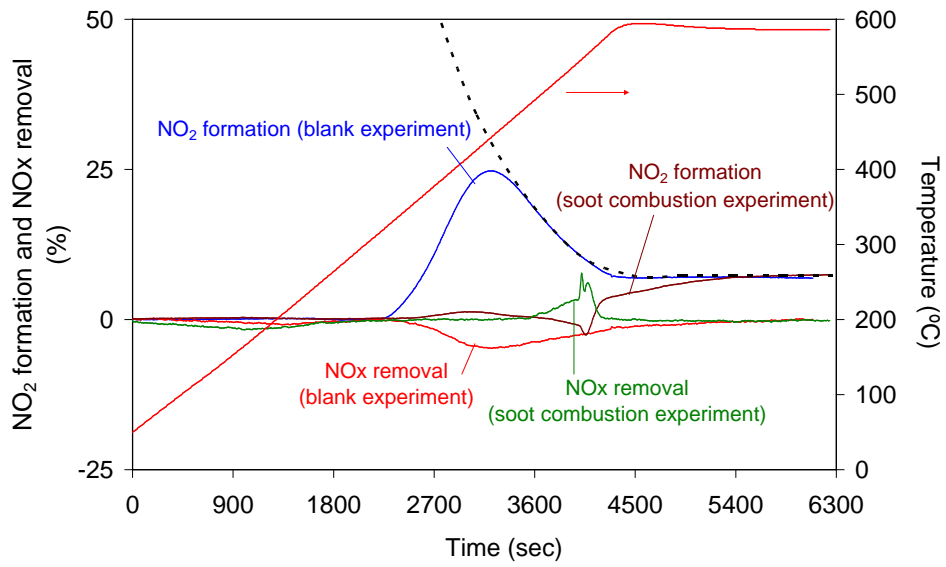
Figure 7



581
582
583
584

585
586
587
588
589
590
591
592

Figure 8



593
594
595